Ecological Indicators 110 (2020) 105858

Contents lists available at ScienceDirect

Ecological Indicators

journal homepage: www.elsevier.com/locate/ecolind

Subsurface chlorophyll maxima in the North Eastern Arabian sea: Simulation on impact of warming

H. Midhun shah[a,*], B.R. Smitha[b,*], A.A. Mohamed Hatha[a,*], M. Sudhakar[b]

[a] Department of Marine Biology, Microbiology and Biochemistry, School of Marine Sciences, Cochin University of Science and Technology (CUSAT), Kochi 682016, Kerala, India

[b] Centre for Marine Living Resources and Ecology (CMLRE), Ministry of Earth Science, Kochi-508, Kerala, India

ARTICLE INFO

Keywords:
Stratification
SCM
Bio-Argo floats
North Eastern Arabian Sea
Settling velocity

ABSTRACT

Stratified tropical oceanic systems are in general observed with Subsurface Chlorophyll Maxima (SCM), which was identified as light adaptation of shade-loving picophytoplankton groups. Apart from the light adaptation strategies of phytoplankton, the physical properties of water masses have significant role to hold the phytoplankton in particular layers. The present study gives theoretical explanation on the influence of fluid properties of water on the settling velocities of micro-nano phytoplankton groups, which contribute the SCM. The data and samples were collected from North Eastern Arabian Sea (NEAS) during March (Spring Inter Monsoon), by means of Bio-Argo floats, CTD and remote sensing. The analysis gives indications to the possible strengthening of SCM in the scenario of warming and enhanced stratification. The study conducted simulations using basic stoke's equations on most abundant species of the area and found that the fluid density has a significant role in the settling of non-motile, suspended phytoplankton groups, irrespective of their cellular density. The simulations show strong decelerations at the same depths, in the upper part of the pycnocline but with varying settling velocity. A numerical expression derived based on curve fitting and multiple regression analysis substantiates the influence of vertical density on SCM. The sensitivity analysis (Global sensitivity Analysis) indicates warming trend in NEAS strengthening the stratification, which in turn influences the concentration in SCM and is capable of altering the primary production.

1. Introduction

Subsurface chlorophyll maxima (SCM) are a ubiquitous feature of the ocean and are very common in tropical and subtropical waters. This submerged biological feature contributes significantly to the column primary production with distinct variations in time and space. SCM get influenced by the prevailing physical processes, mixing, stratification (density), and the phytoplankton group that contributes to the maxima layer. Globally, many studies have attempted to explain the occurrence, dynamics, influence on the SCM due to the predominant ecosystem processes and the ecological implications due to this enhanced concentration of phytoplankton. Among these, the most notable explanation is the preference of certain shade-loving organisms resulting high abundance in the subsurface (Falkowski, 1980; Wang et al., 2016) or photo-acclimation (Fennel and Boss, 2003). Another accepted version is the adaptation of phytoplankton with low cell settling velocity to utilize diapycnal nutrient fluxes in these low light levels (Moore and Villareal, 1996). Biologically, maxima of phytoplankton biomass occur where the growth rate is balanced by respiration (loss) and the variation in sinking velocity. Thus, buoyancy of the phytoplankton cells is a major factor regulating the depth of their distribution, which is a function of water density and cell volume (Macías et al., 2013; Moore and Villareal, 1996).

A number of studies have been carried out on SCM of the Arabian Sea; the explanation of the role of tiny organisms, viz., the pico (Jochem, 1995) and nano components. Derivation of embedded maxima in vertical chlorophyll from satellite data (Matondkar et al., 2006), and time-space variation in the SCM (Ravichandran et al., 2012) at the EAS based on bio-Argo float's profiles, have been the major contributions in the recent decade. Observations from various sources explain the occurrence of chlorophyll maxima at a 40–100 m depth column with significant seasonal variations. Accordingly, the level of

* Corresponding authors at: Department of Marine Biology, Microbiology and Biochemistry, School of Marine Sciences, Cochin University of Science and Technology (CUSAT), Foreshore Road, Kochi 682016, Kerala, India (H. Midhun shah and A.A. Mohamed Hatha); Centre for Marine Living Resources and Ecology, Ministry of Earth Sciences, LNG Road, Ochanthuruth, Puthuvype, Kochi-682508, Kerala, India (B.R. Smitha).

E-mail addresses: mishahueco@gmail.com (H. Midhun shah), smitha.br@gmail.com (B.R. Smitha), mohamedhatha@gmail.com (A.A. Mohamed Hatha).

https://doi.org/10.1016/j.ecolind.2019.105858
Received 20 May 2019; Received in revised form 9 September 2019; Accepted 22 October 2019
Available online 07 November 2019
1470-160X/

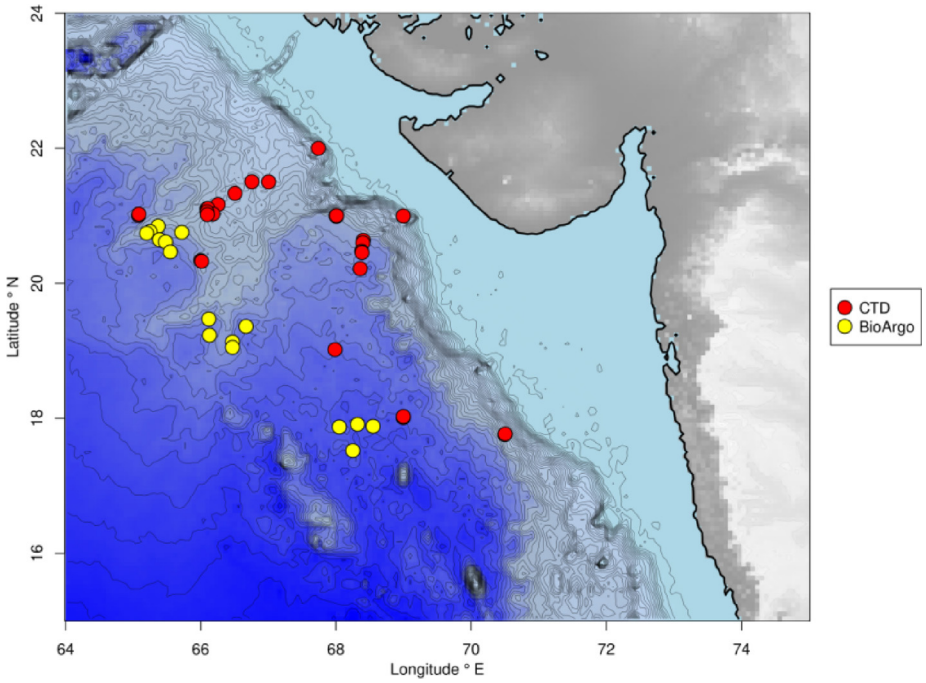

Fig. 1. Study area showing the locations of field sampling (Red dots) and Bio-Argo floats (Yellow dots).

occurrence of the maxima associated with the euphotic depth and variation in biomass was reported to be related to the vertical oscillations in Rossby waves owing to its association with thermocline (Ravichandran et al., 2012). Density stratification ascribed to warming acts as a barrier, which limits the vertical exchange of dissolved inorganic substances resulting in the retention of nutrient-rich waters within the subsurface. The microbial community appears to be more versatile in these subsurface low light (LL) ecotypes (Buitenhuis et al., 2012; Jochem, 1995) and the regenerated nutrient regimes, resulting in their abundance. During inter-monsoon, light is available for photosynthesis in the Arabian Sea in abundant even to the deep thermocline (Hay et al., 1993; Krey, 1976) (Brock et al., 1993). The higher light penetration during the month of March (Hay et al., 1993; Krey, 1976) resulted in abundance of *Synechococcus* and pico-eukaryotes (Jochem, 1995), whereas *Prochlorococcus* is ubiquitous with minor fluctuations. Seasonal processes of the region, especially the degree of vertical mixing is relatively weak during Spring Inter Monsoon (SIM), and it is evident with a strong and well-defined SCM. Also, the season is associated with widespread blooming of *Noctiluca* at surface (Gomes et al., 2008). According to recent studies, (Lotliker et al., 2018; Rosario Gomes et al., 2009) the bloom intensity and its spread, are intensifying due to warming. Therefore, the warming has a significant impact on bio-geochemical processes in NEAS, which even extends to the deep column due to biological pumping, influencing the perennial OMZ, with possible impact on the regional mesopelagic ecosystem.

At present, major studies on SCM are based on two assumptions, (1) Shade-loving - picophytoplankton and picoeukaroytes, which have a distribution throughout the water column, but contributes to SCM on their optimal light and (2) Photo-acclimation, which seems to be similar to shade-loving, but these organisms have a wide range of light adaptation and forced to withstand at low light intensity. Diatoms and less motile dinoflagellates contributed more to this category. The first category mostly docked below 100 m, and commonly called as Deep Chlorophyll Maxima (DCM). The second category related to the upper layers of ocean, and closely related to Mixed Layer Depth (MLD). In these, the photo-acclimation of surface phytoplankton to subsurface layers is less studied in NEAS. To describe the stratified system of NEAS, the work was conducted during March, the initial month of SIM.

The present study explores the possible role of the physical structure of water masses for photo-acclimation resulting in the formation of SCM. The phytoplankton groups such as diatoms and dinoflagellates have a wide range of light adaptability to adjust in response to the physical settings. A similar study by Fennel and Boss (2003), on Crater Lake, where the pycnocline is weak, suggests that small cells in less stratified waters do not contribute to SCM by settling; instead it occurs at the depth where growth and respiration compensate. It is assumed that the fluid dynamics of the regional water mass regulates the settling of phytoplankton, over the adaptation strategies of various phytoplankton groups to form SCM. SCM are more associated with stratified waters, which is getting stronger due to warming. Specifically, this study is an attempt to explain how the fluid dynamics influence the depth of settlement of surface phytoplankton groups in stratified waters thus explaining the potential impact of warming in biological systems.

2. Methodology

2.1. Data sources

The main sources of data sets used for the study are vertical profiles from Bio-Argo floats, which measures chlorophyll in addition to temperature, salinity and dissolved oxygen. The floats were deployed in the North Eastern Arabian Sea by INCOIS, India. The available data-sets were pooled from four different Argo floats (2902091, 2902092, 2902093 and 2902118) from the spatial domain of 17–20 °N and 66–70 °E in the NEAS. The temporal span of Bio-Argo floats are different and mostly it varies from three months (2902091) to three years (2902092). But some floats (2902093 and 2902118) considered in this analysis are still active. The authors selected Bio-Argo float's profiles for March 2013 to validate the data with the 29 CTD profiles (SBE 911 Plus) collected during cruise 314 of *FORV Sagar Sampada* conducted during March (Fig. 1). The CTD system is equipped with auxiliary sensors of dissolved oxygen, fluorescence and photosynthetic active radiation (PAR)

Each Bio-Argo floats provide approximately four profiles during the study period, giving a total of 16 profiles during March 2013. The Bio-Argo floats were programmed to collect profiles at noon. The accuracy of the temperature, salinity, pressure, chl-*a*, and dissolved oxygen concentration measured by these floats were 0.002 °C, 0.005 psu, 2.4

decibars, 0.02 mg m^{-3}, and 8 mM, respectively (Ravichandran et al., 2012). SCM was observed in most of the profiles and the depth of occurrence was well within the euphotic column. As a proxy to the active euphotic column, profiles up to 100 m depth only were considered for the analyses. Ancillary parameters, which regulate the vertical chlorophyll distribution, were extracted from remote sensing data sets. Shortwave radiation (swr) was taken from the TropFlux net from *www.incois.gov.in*, Eastward/Northward wind speed from ASCAT DATA Products (Daily) from www.incois.gov.in, and Photosynthetically Active Radiation (PAR), R. Frouin (Ocean Colour Monitor, Level-3 product) from Aqua MODIS.

2.2. Data analysis

To consider column properties of the Chl-*a* distribution, all the profiles were subjected to curve fitting, making use of the 'nls' (nonlinear least squares) package in R programming language, and the data points were fitted with a Gaussian curve with 97 degrees of freedom. A Gaussian function is a characteristic symmetric "bell curve" shape or a Normal distribution curve that quickly falls off towards plus/minus infinity.

As per the present analysis, the fit extracted is

$$f(x)=Chl_{max}e^{\left[\frac{(-D-D_{max})}{Chl_{spd}}\right]^2} \quad (1)$$

where D = [1–100]; 100 m being the proxy for the euphotic depth. SCM occupies within 100 m depth for the whole profiles. The coefficient Chl_{max} denotes the peak chlorophyll, D_{max} the depth of occurrence of the maxima and Chl_{spd} is the spread of the SCM. The coefficient Chl_{max} is highly varying and is a significant character of SCM. On the other hand, Chl_{spd} considers the spreading of chl from its peak Chl_{max}. Profiles from Bio-Argo floats and CTD were treated separately for the coefficients (Chl_{max}, D_{max} and Chl_{spd}) which determine intensity, depth of maxima and spread. The Principal Component Analysis (PCA) also considers these derived coefficients, to explain the contribution of each factor for characterizing the SCM profiles as well as to delineate the forcing variables.Further, a refined mathematical model is derived from the coefficients extracted and the model efficiency was tested using Global Sensitivity Analysis (GSA).

2.2.1. Variable syntheses for the study

The variables were categorized as surface parameters, SCM parameters and atmospheric components, in which surface parameters are selected from the depth of 5 m, and SCM parameters, are extracted from depth where SCM was observed. The parameters taken are shown in the Table 1.

The PCA was done using R scripts utilizing ade4 (Analysis of ecological data: Exploratory and Euclidian methods in environment) package (Dray and Dufour, 2007) with visualizations using Factoextra package (Kassambara and Mundt, 2017). Mixed Layer Depth (MLD) was derived from the change in density gradient from 5 m level of the stable surface to the depth at which density increase by 0.03 (de Boyer Montégut et al., 2004). The equation used in the study is as follows:

MLD = depth where $t = \sigma t_{5m} + 0.03$ kg. m^{-3} and is represented in meter.

The settling velocity and distribution of the organisms in the euphotic column is explained using the Stock's equations of fluid dynamics (Bach et al., 2012). Stock's equations were implemented as a function of water mass (fluid density) and phytoplankton cell density. Considering stability and density, simulation analyses on settling velocity were done on the most dominant/relevant species of the region/season. Details on the phytoplankton species considered were referred from *FORV Sagar Sampada* old cruise repository. The derived seawater properties such as water mass densities and buoyancy frequencies were extracted using "gsw" (Gibbs Sea Water) package (Kelley and Richards, 2017) in R from the vertical profiles. Phytoplankton cell densities were calculated using secondary data-sets refereed from the works of Harrison et al. (2015) with a focus on the bottom-up drivers and physical properties.

Table 1
List of parameters.

Symbol	Parameter	Unit
sali.surf	Surface salinity	psu
temp.surf	Surface temperature	°C
fluro.surf	Surface chlorophyll	mg m^{-3}
oxy.surf	Surface oxygen	mM
sigma.surf	Surface density	kg m^{-3}
sali.scm	SCM salinity	psu
temp.scm	SCM temperature	°C
fluro.scm	SCM chlorophyll	mg m^{-3}
oxy.scm	SCM oxygen	mM
sigma.scm	SCM density	kg m^{-3}
swr	Shortwave radiation	W.m^{-2}
par	Photosynthetic Active Radiation	Einstein. m^{-2} day^{-1}
wind	Wind stress	pa
mld	Mixed Layer depth	m
a, b and c	Gaussian parameters	–

3. Results and discussion

The characterization of chlorophyll profiles using Gaussian function explains the distribution of peaks and shows appreciable homogeneity throughout the month (Fig. 2). Earlier studies records that the vertical distribution of Chl-*a* and its dynamics are mainly controlled by nutrient flux, photo-acclimation of phytoplankton, and grazing (Behrenfeld and Boss, 2014; Cullen, 2015; Huang and Xu, 2018; Huisman et al., 2006).

Light adaptation is a strong reason for SCM (Brock et al., 1993), but the response of which varies between species, and there is a possibility for multiple peaks of chlorophyll. In contrast, the profiles examined in the current study showed well-defined single peaks in general, which indicated the influential role of factors other than a light adaptation of the phytoplankton community. The organismal light tolerance levels (Bacillariophyceae: 6.4–84 μEm^{-2}s^{-1}, Dinophyceae: 6.6–46 μEm^{-2}s^{-1} and Cyanophyceae: 5–38.8 μEm^{-2}s^{-1}) as experimentally recorded by

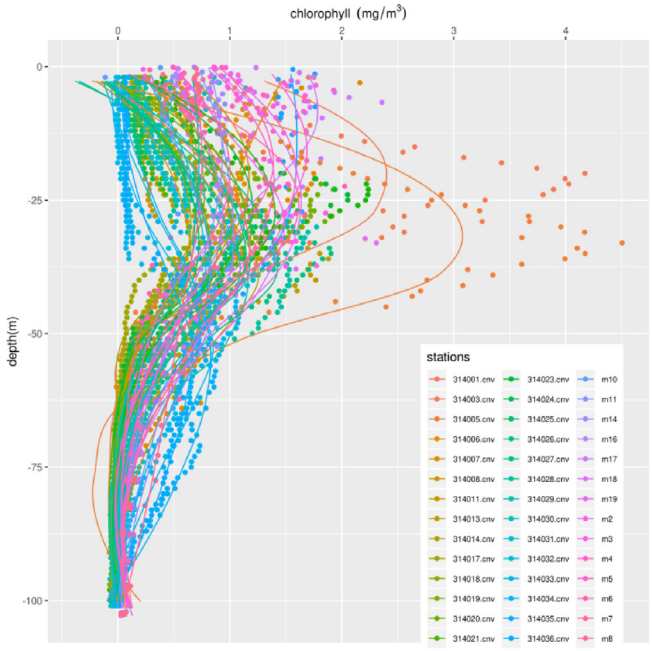

Fig. 2. The characterization of vertical chlorophyll profiles from FORV Sagar sampada (Cruise 314) and Bio-Argo floats using Gaussian function.

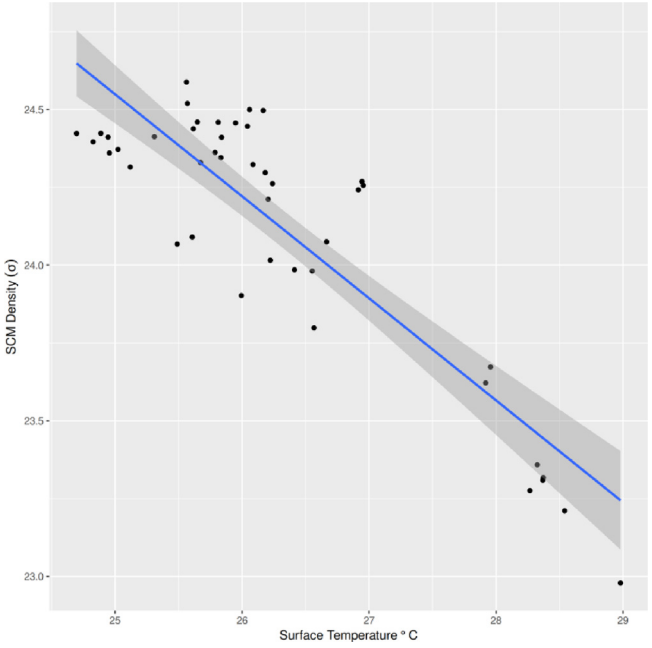

Fig. 3. Inverse correlation of Sea Surface temperature and subsurface density.

(Brock et al. 1993) and the phytoplankton community having almost similar composition and PAR in the study region as observed by Jochem (1995) supports this speculation.

To explore the role of other factors, the Gaussian coefficients of profiles extracted were made to correlate with the possible surface and SCM hydrodynamic parameters. The temperature in the SCM (temp.scm) varies from 24.05 °C to 28.9 °C, and is comparable with the regional SST (temp.surf) (24.69 °C – 28.98 °C). The data sets did not show any significant correlation between surface and subsurface parameters except with the SCM density (sigma.scm) and SST (temp.surf) (Fig. 3).

The SCM density and SST have a strong inverse relation with an R^2 of 0.77 and have a significant p-value (< 0.005). PAR decreases exponentially to the deep layers but observed to be within the range that sustains diatom/dinoflagellate species and at the optimum level to accommodate cyanophyceae, indicating that light is not a limiting factor for either of the groups (nano and pico). According to the PAR levels (1.68–54.69 $\mu Em^{-2}s^{-1}$) observed in the SCM, it could be inferred that a mixed community of phytoplankton groups persists in the system (Jochem, 1995). The concentration of the limiting nutrient such as silica shows indications of the presence of diatoms. The vertical distribution of silica (SiO_4) was observed to be low (0.12 μM) from the surface to subsurface (40 m) and getting increased (2.52 μM) below the SCM, indicating the presence of diatom up to the subsurface. The vertical distribution of silica is found to be in supportive of the observation from Banerjee and Prasanna Kumar (2014) explaining the aeoline nutrient deposition which is minimal during SIM.

The PCA indicates a significant role of SST (temp.surf) on subsurface density (sigma.scm). The Gaussian coefficients derived from chlorophyll profiles (a = Chl_{max}, b = D_{max} and c = Chl_{spd}) were found to be influenced by multiple parameters, and also doesn't indicate any direct relation to phytoplankton physiology due to increase in temperature (Fig. 4). However, the coefficient 'c' = Chl_{spd} (the spreading factor) has a direct correlation with MLD, which is associated with nitracline (Gardner et al., 1999); layer which has greater significance in recharging SCMs by providing nutrients. The multiple factors controlling the chlorophyll peaks are well delineated in the PCA bi-plot (Fig. 4). The bi-plot showed the factored SCM scores as high peak (hp), peak (p), and low peak (lp). The single 'lp' value is found to be associated with 'c' and MLD, whereas hp and p are significantly influenced by the SCM

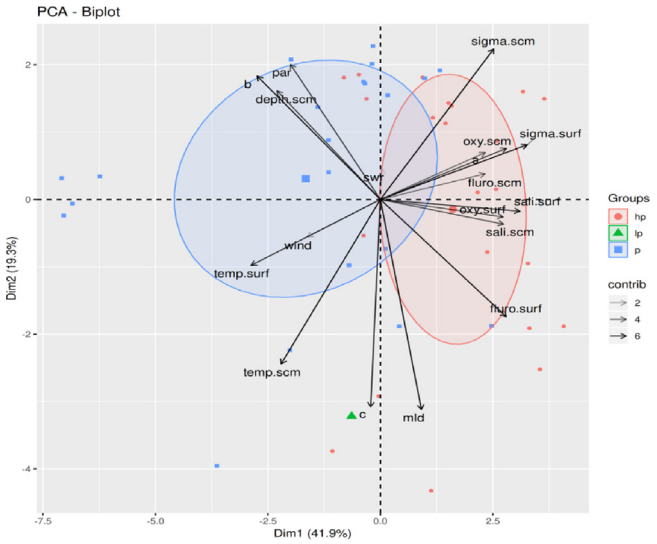

Fig. 4. The Bi-plot showing Principal Components (PC) of hydrographic parameters and Gaussian coefficients.

temperature (temp.scm) and density (sigma.scm). Further, 'hp' is related to density variability and 'p' with deeper depths.

3.1. Light requirements and vertical inclinations

The innate biological factors regulating the SCM vary from species to species, and it depends on community composition of phytoplankton groups. The light intensity has a great influence on specific growth rates of phytoplankton. Previous reports show that photo-inhibition of natural phytoplankton in surface water are more dependent on the quality and intensity of light availability (Richardson et al., 1983). Optimal PAR for the growth of cyanobacteria (Blue-green Algae) is between 5 and 39 $\mu Em^{-2}s^{-1}$ (Richardson et al., 1983), and they mostly are shade loving. Dinoflagellates being locomotive perform diel vertical migration in response to light, to maintain in shade during bright sun hours. These organisms accumulate in the subsurface to form SCM, as reported by Dodge and Hart-Jones (2009); Harris et al. (1979) and Hasle (1950). In contrary to Dinoflagellates and cyanobacteria, diatoms have a wide range of light adaptation (Valiela, 1995). The variability in the light-harvesting efficiency arises due to the pigment composition of individual groups (Jeffrey et al., 1997). The in-situ PAR at SCM, which was observed to be significantly strong during March, was found to be in the optimum level (6–84 $\mu Em^{-2}s^{-1}$) to sustain diatom (Fig. 5) from the 29 profiles of in-situ PAR from CTD attached sensor.

However, there was no significant relation with chlorophyll maxima and the PAR at SCM. The uncorrelated parameter draws attention towards the physical setting of water mass, which contributes to the formation of chlorophyll maxima in the subsurface. The main question to address in the study is whether the water mass density or the light adaptation strategies of phytoplankton influence the vertical inclination of Chl-*a*.

The influence of vertical density gradient on SCM is substantiated by comparing the linear and nonlinear regressions (curve fitting) of averaged vertical profiles of chlorophyll with main forcing variables such as PAR, depth, and density (σt) of water mass. Similar to chlorophyll profiles, the forcing variables show generalized Gaussian function, except the PAR-chlorophyll relation (Fig. 6). The coefficients derived are shown highly significant (97 degrees of freedom). The PAR was observed maximum at the surface, whereas the density to chlorophyll relation was found to be strong at subsurface in 20–60 m range. The SCM peak (Chl_{max}) is more proximate to density maxima than the PAR and indicated as 'p' and 'q' in Fig. 6.

As the individual profiles have non-linear relations with chlorophyll

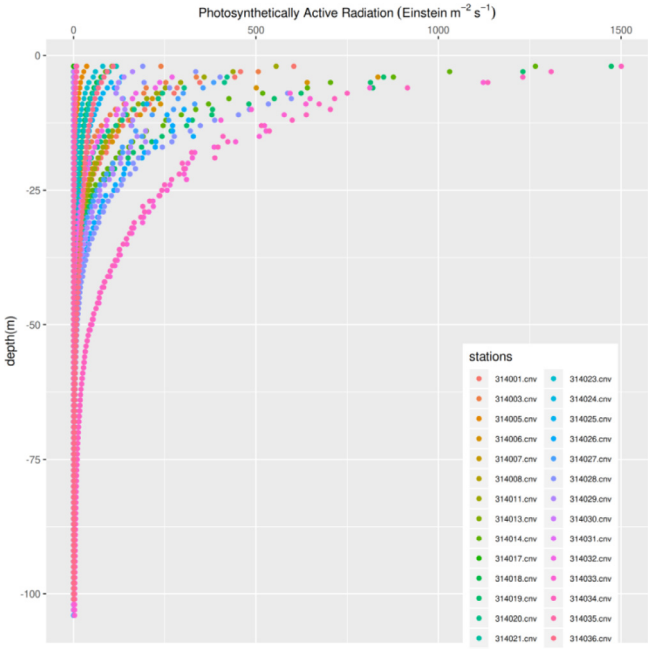

Fig. 5. In-situ PAR vertical distribution from FORV Sagar sampada (Cruise 314).

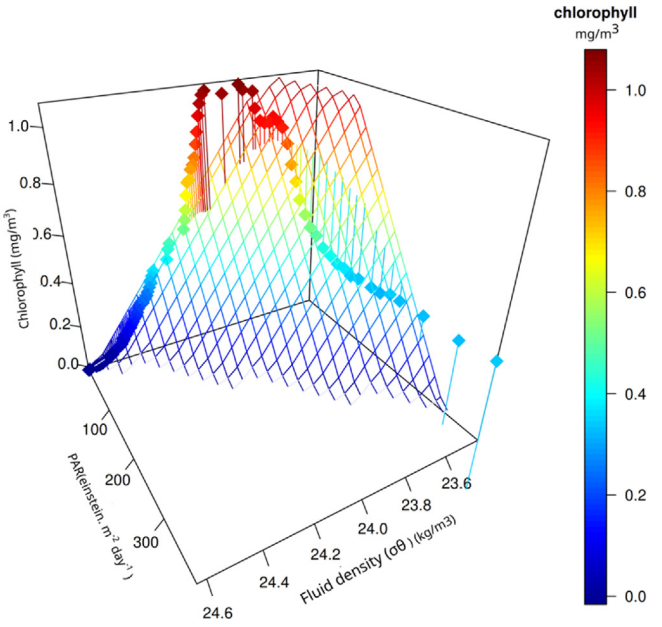

Fig. 7. Multiple regression analysis of chlorophyll, sigma-theta, and PAR.

profiles, a multiple regression analysis was devised, which has a significant fit with an R^2 of 0.7 with a p-value of 2.2e−16 (Fig. 7). The multiple regression analyses were done with PAR and density as predicting variables, where the density shows similar p-value with PAR (2.2e−16). This again accounts for the fact that density has an influential effect on SCM.

3.2. Phytoplankton settling velocity

Model by Fennel and Boss, (2003) suggests that maxima in phytoplankton biomass occur at "general compensation depth", where the growth rate is balanced by losses due to respiration and grazing or the divergence in sinking velocity. It is also found that divergence in sinking velocity could be introduced by a change in water density, and concluded that density changes at pycnocline in natural environments are too small to contribute to the above balance in a significant way. However, the present study shows that density changes in the upper layers are considerably strong and are influential to the sinking rates of suspended particles. The sinking rates of phytoplankton groups vary, owing to the size, shape, as well as the inertial interaction due to dragging. This determines the distribution of the less-motile phytoplankton in the non-turbulent photic zone. But this structure was

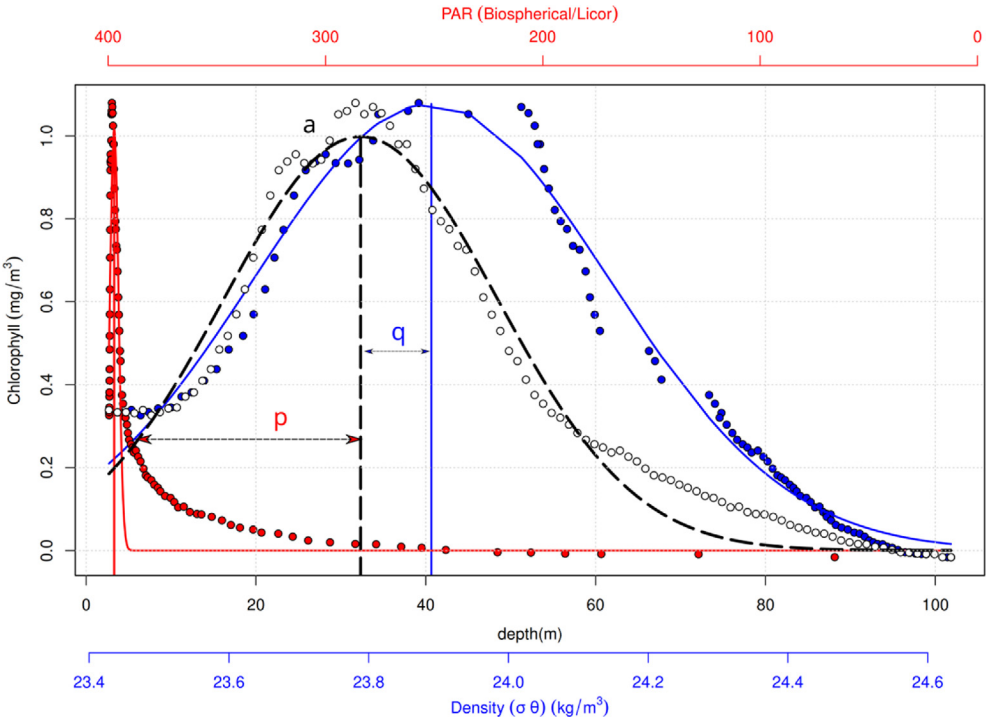

Fig. 6. Curve fittings of vertical chlorophyll, sigma-theta and PAR.

altered when the density of fluid is greater than the density of phytoplankton, which results the organism to be buoyant for a particular period.

3.3. Simulations on fluid interactions

As per the stable sea conditions (March/spring), particle sinking or phytoplankton settlement can be well explained by Stokes Theorem. If a particle is influenced by its own weight while falling through a fluid, its terminal velocity will be constant when the sum of the dragging and buoyant forces on the particle exactly balances the gravitational force. According to this, the sinking rate of a particle (spherical) in a viscous fluid (μ) is

$$V = \frac{1}{18\mu} d^2 g(\partial_s - \partial_f) \tag{2}$$

where d is the diameter of the particle and g is the acceleration due to gravity, in which ∂_s and ∂_f are the density of suspended particle and fluid respectively. The constant 1/18 in the equation is derived by simplifying Reynolds's no of the sphere. The phytoplankton dimensions taken for the study were based on equivalent spherical diameter (ESD) as described in Harrison et al. (2015)

Phytoplankton maintains buoyancy by its innate mechanisms of gas vacuoles and lipids, and often heavier than seawater. The buoyancy of phytoplankton is defined by the volume rather than mass, which depends on respiration and photosynthesis. This disproportion in mass and volume makes the phytoplankton (especially diatoms) positively buoyant after a critical size range (Gross and Zeuthen, 1948).

Considering the phytoplankton cells (density = ∂_p) sinking in seawater (density = ∂_f) with gravitational pull (g) and kinematic viscosity (μ). If cells are assumed to be spherical (Reynolds no < 1), the velocity of sinking rate on the plankton cells are mainly determined by the differences in cell density (∂_p) and seawater density (∂_f).

When $\partial_p > \partial_f$ then the equation becomes

$$V = \frac{1}{18\mu} d^2 g(\partial_d) \tag{3}$$

Where ∂_d *is* the density difference of fluid and phytoplankton cells.

When ∂_d is positive, the cells will sinks.

When $\partial_p < \partial_f$, the equation becomes

$$V = \frac{1}{18\mu} d^2 g(-\partial_d) \tag{4}$$

The negative density difference ($-\partial_d$) decelerates the cells.

3.4. Model insights and considerations

The sinking rate is different for various organisms as it is determined by the shape, and it differs from species to species. The shape changes the effects by changing Reynolds numbers, and eventually, the pattern of sinking is uneven to predict. From the previous studies of sinking rates, it is found that for very large-sized cells with Reynold's numbers up to 2.01, Stoke's law is inapplicable. However, phytoplankton size groups having less than 200 μm are appropriate to consider for Stoke's equation (Moore and Villareal, 1996). The major difference between (4) and (5) arises due to the difference in hydrodynamics, especially the stability of the water column for similar species. This is well captured in the Brunt Vaisala (BV) frequency of the water column (Fig. 8).

$$N^2 = -\left(\frac{g}{\partial}\right)\frac{d\partial}{dz} \tag{5}$$

where g acceleration due to gravity, ∂ is potential density and $d\frac{\partial}{dz}$ is the change in density with depth.

In March, BV shows close existence with chlorophyll maxima and being a quiescent season, MLD is generally thin and is more or less

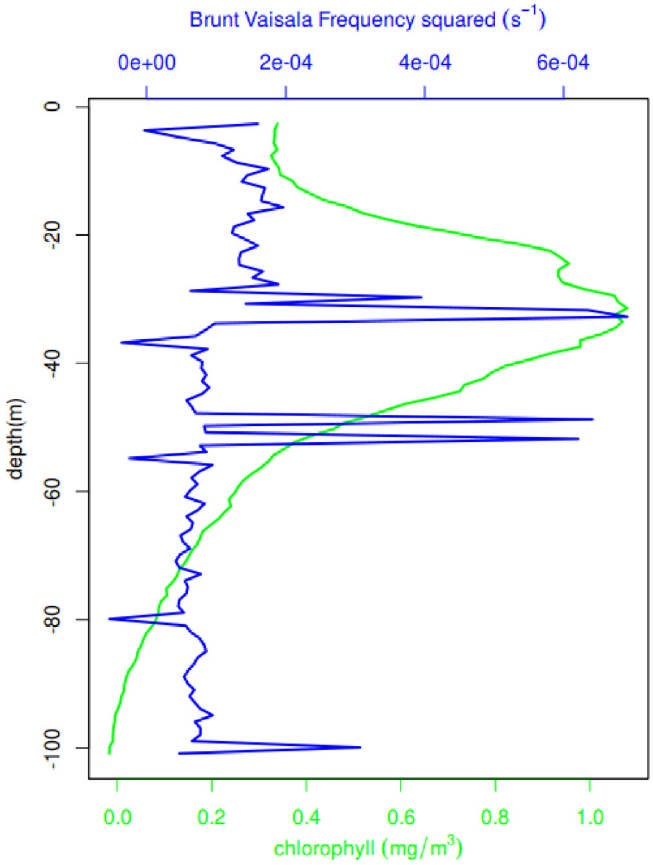

Fig. 8. Subsurface chlorophyll maxima and Brunt Vaisala (BV) frequency.

associated with the pycnocline. The depth of occurrence of SCM during March, being the layer just above the pycnocline, indicates the significance of this gradient layer to the phytoplankton accumulation depth.

To explain this co-occurrence in detail, the settling of particles was simulated using the generalized Stokes equation for 10 most relevant and commonly occurring species of the region (from the database of *FORV Sagar Sampada*) (Table 2). As the NEAS system is usually dominated by diatoms, the analysis considered nine abundant diatom species and one dinoflagellate: *Noctiluca scintillans*, which is a prominent blooming species in the region. Further analyses were done using four representative species such as *Thalassiothrix longissima*, *Guinardia striata*, *Nitzschia longissima and Noctiluca scintillans which were* frequently observed during the study period (Fig. 9).

Necessary input parameters for simulation, most importantly, the cell volume and biomass in carbon for the derivation of cell density were obtained from Harrison et al. (2015). The kinematic viscosity (μ) was derived from the hydrographic profiles from Bio-Argo floats during March 2013, and the observations indicated strong density gradient in the upper layer (Fig. 10. 5). All the species selected for the simulation showed a strong deceleration from the depth of 20–40 m, irrespective of their volume, carbon content, density and diameter (Fig. 10-1, 2, 3 and 4).

The analysis indicates that sinking rates of phytoplankton cells in a fluid system of strong density gradient are totally governed by fluid density, and influence the terminal velocity, which is minimal at subsurface. The simulated settling velocities, assuming the system as laminar/streamline flow, range from -3.229×10^{-06} m/s to -2.384×10^{-13} m/s (negative sign indicates deceleration). This indicates that the stratified water column sustains phytoplankton groups of a wide range of light adaptability.

Table 2
Dimensions of abundant phytoplankton species from study area.

Sl. No	Species	Abundance** (No.s/L)	Volume* (μm^3)	Carbon* (Pg C/ cell)	Volume in m^3 (SI)	Carbon in kg (SI)	Diameter (m) (SI)	Density in Kg/m^3 (SI)
1	*Chaetoceros diversus*	95	374	38.7	3.74E-16	3.87E-12	2.00E-11	1.03E-14
2	*Dactyliosolen fragilissimus*	164.5	8300	337	8.30E-15	3.37E-11	1.58E-10	4.06E-15
3	*Ditylum brightwellii*	74	73,400	2340	7.34E-14	2.34E-10	6.75E-10	3.19E-15
4	*Eucampia zodiacus*	56	9150	441	9.15E-15	4.41E-11	1.68E-10	4.82E-15
5	*Guinardia striata*	222	35,700	1290	3.57E-14	1.29E-10	4.17E-10	3.61E-15
6	*Nitzschia longissima*	268	599	43.4	5.99E-16	4.34E-12	2.73E-11	7.25E-15
7	*Noctiluca scintillans*	1531	83,700,000	316,000	8.37E-11	3.16E-08	7.36E-08	3.78E-16
8	*Thalassionema frauenfeldii*	89	1500	106	1.50E-15	1.06E-11	5.04E-11	7.07E-15
9	*Thalassionema nitzschioides*	58	1240	63.4	1.24E-15	6.34E-12	4.44E-11	5.11E-15
10	*Thalassiothrix longissima*	205	13,500	422	1.35E-14	4.22E-11	2.18E-10	3.13E-15

** Abundance calculated from *FORV Sagar sampada* database.
* From Harrison et al. (2015)

3.5. Spring Inter- Monsoon (SIM) a perfect scenario for SCM

Present analyses exclusively focus on the process in the month of March, which is an ideal period for persistent shallow SCMs, due to weak wind forcing and high irradiance. March is the transition phase from a highly productive system to a less productive stratified system and variations in temperature are also important. Being the most stable and stratified period of the year, applications of Stoke's equations for explaining the settling of organisms can be appropriately used to describe the water mass-phytoplankton density relationship and depth of settlement. Prior months (Winter Monsoon) of SIM are well mixed due to the winter cooling and convective mixing (Kumar et al., 2001; Prasanna Kumar and Prasad, 1996). Also, the subsequent season (Summer Monsoon) is turbulent due to heavy wind stress by the monsoon.

Time series analysis of temperature during March gave an indication to the warming of the surface layer with a positive trend (25.29 °C to 26.51 °C) in recent years (Fig. 11). The anomalous hike (27.17 °C to 28.82 °C) observed in 2010 can be explained as a response of the strong El-Nino (Kim et al., 2011). Overall, the temperature increased from the first week (24 °C) to the fourth week (27 °C) over the decade. Temperature variability is very critical in this transition phase and is well correlated with the recurring bloom events in the month. The MLD ranged from 18 m to 87 m throughout the year, and for March the MLD is thin of an average depth of 38 m compared to other months. However, the regional dynamics supports enhanced biological production through recurring bloom events (*Noctiluca*). The depletion of nutrients subsequent to a bloom results in low Chl-*a* on the surface. Conversely, the SCM gets strengthened utilizing the sinking organic matter and the already available nutrients in the subsurface. As explained earlier, the SST has an inverse correlation with subsurface density, which supports them to settle on subsurface. The vertical profiles of density and Chl-*a* for NEAS in the subsequent years too are well evident with the coexistence of SCM and the density gradient (Fig. 12).

The present study has a wider future scope on SCM occurrence and intensity in tropical/subtropical systems, as the warming strengthens the upper ocean stratification (Capotondi et al., 2012), which may further result in an altered production pattern. The observations suggest that SCM closely occur with isopycnal layers of 23.8–23.9 kg/m^3 with a depth range of 40–60 m. The warming of the upper layers contributes to this density gradient and supports the fact that SCM is a strong indicator of warming seas. The increasing chlorophyll maxima values (1.518–3.892 mg/m^3) substantiate the fact that the SCM is strengthening progressively with warming. The density gradient created by warming effectively serves a bottom-up factor in controlling primary

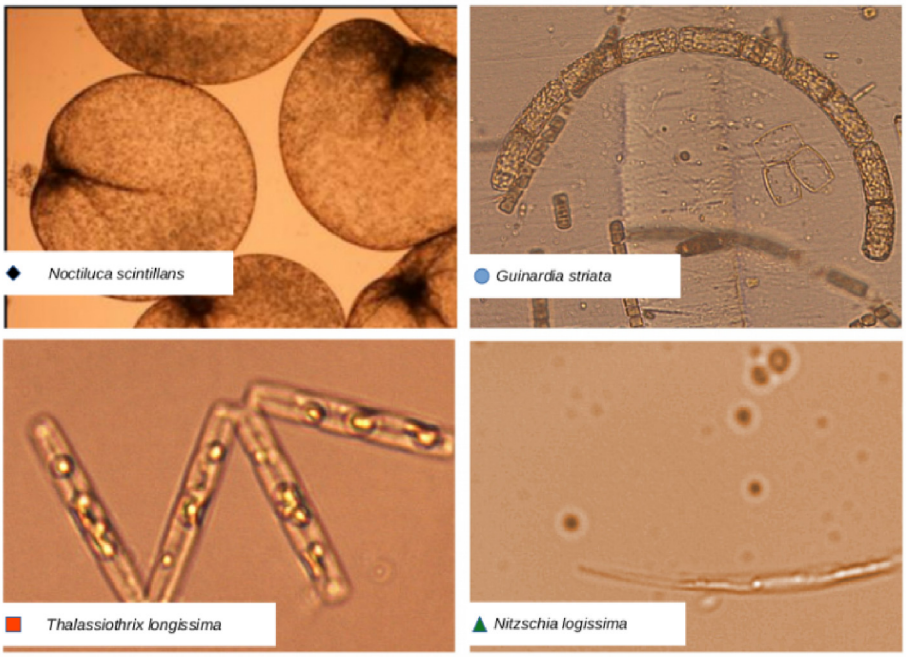

Fig. 9. Prominent Phytoplankton species used for the simulation of settling velocity.

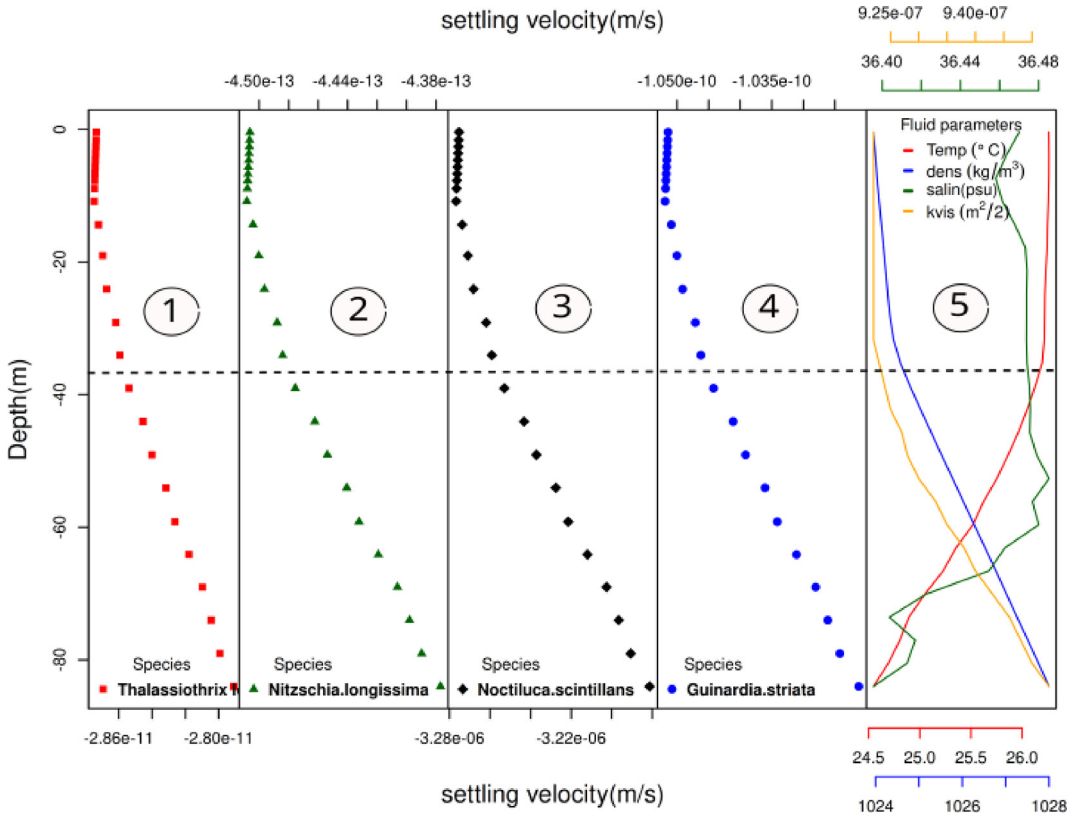

Fig. 10. Settling velocity of four species (1, 2, 3 and 4) showing deceleration after a certain depth. The fluid system (5) shows a strong density gradient in 40 m, where the most probable occurrence of SCM in March is found. The dotted lines (———) show the mean deceleration point.

production in tropical oceans. The NEAS is reported to harbour increased surface production during spring intermonsoon (Goes et al., 2005) and is obviously a carbon sink. As put forward in the present analysis, the increase in temperature and as a result strengthening in stratification may intensify the SCM, boosting the production trend.

3.6. Modeling chlorophyll maxima and Global sensitivity analysis (GSA)

The analysis of the dynamics of SCM shows sigma-t (σt) is the most influencing parameter on chlorophyll maxima than the PAR. The insights are generated by using multiple methodologies such as curve fitting, PCA and multiple regression analysis. To apply these understandings for predictive purposes, a numerical model "*Chloromax*" is

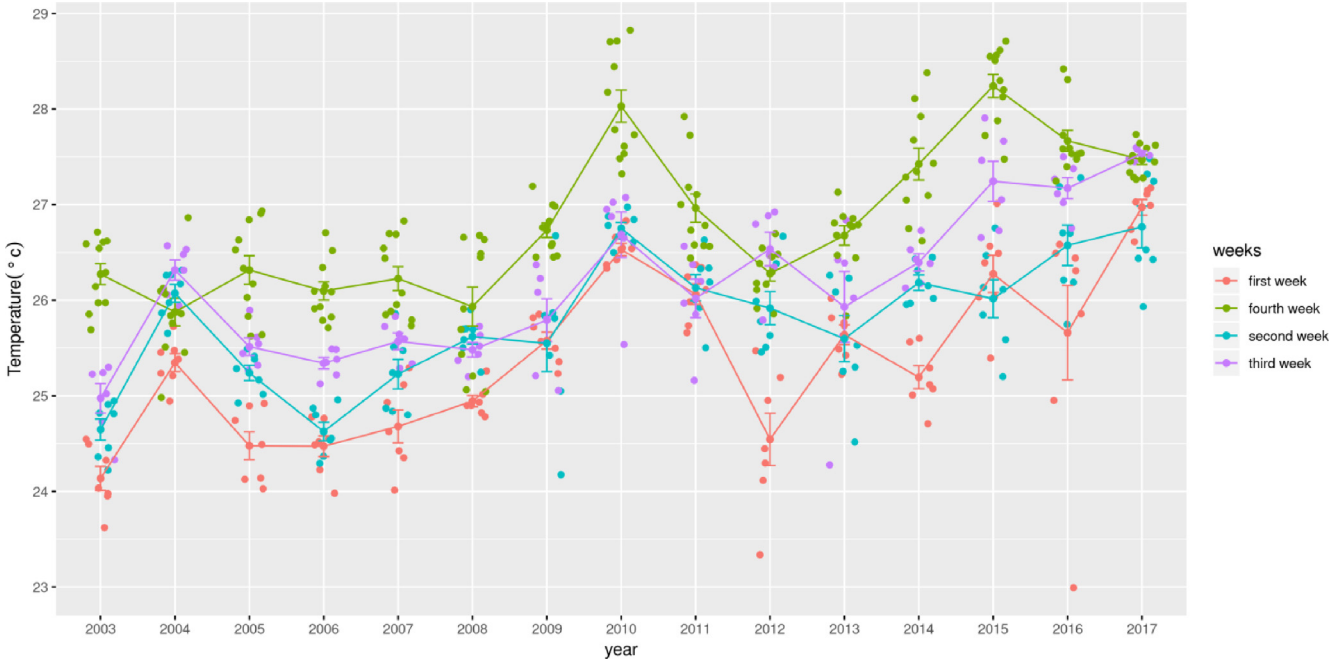

Fig. 11. SST variation in NEAS from 2003 to 2017 March. The peaks observed in 2010 are supposed to be the El Nino effects.

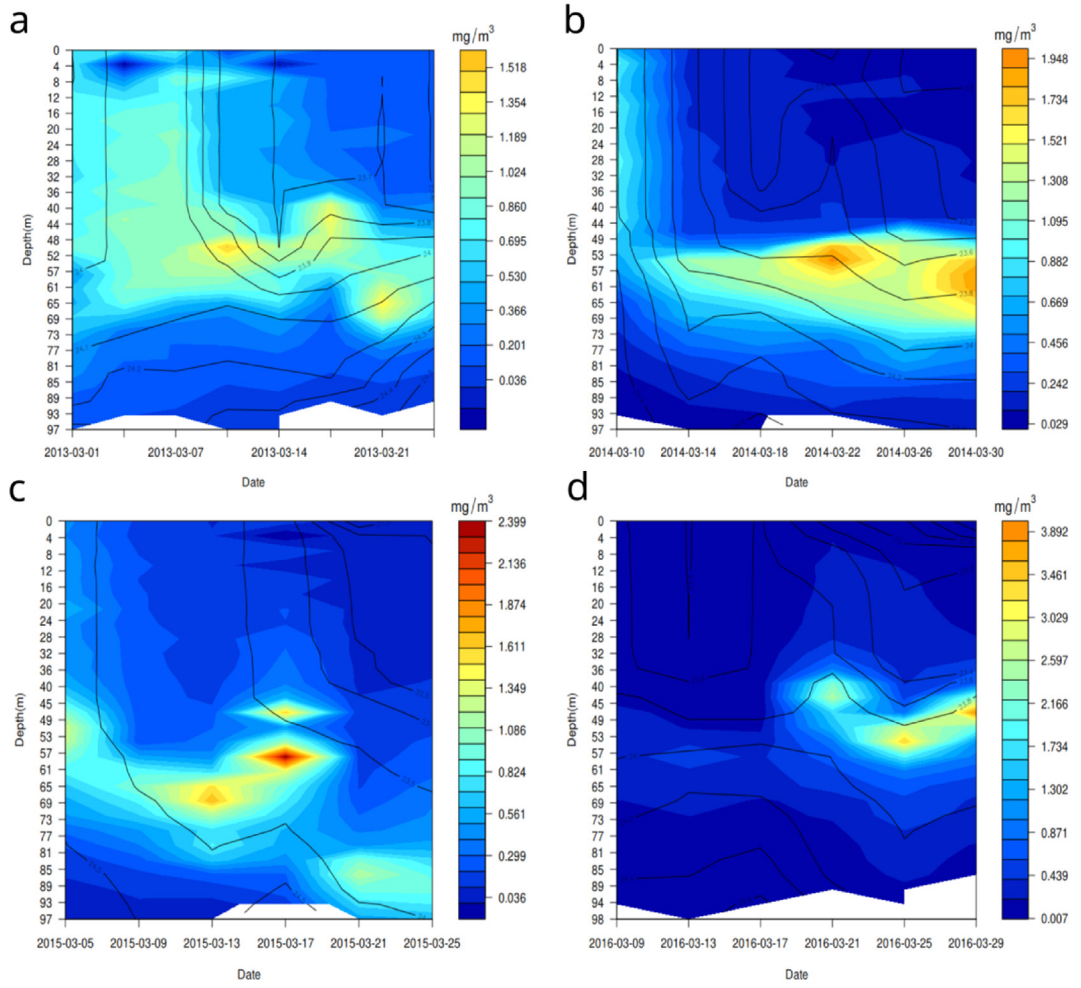

Fig. 12. Density stratification and Subsurface Chlorophyll Maxima (SCM) on various years: a) 2013, b) 2014, c) 2015 and d) 2016.

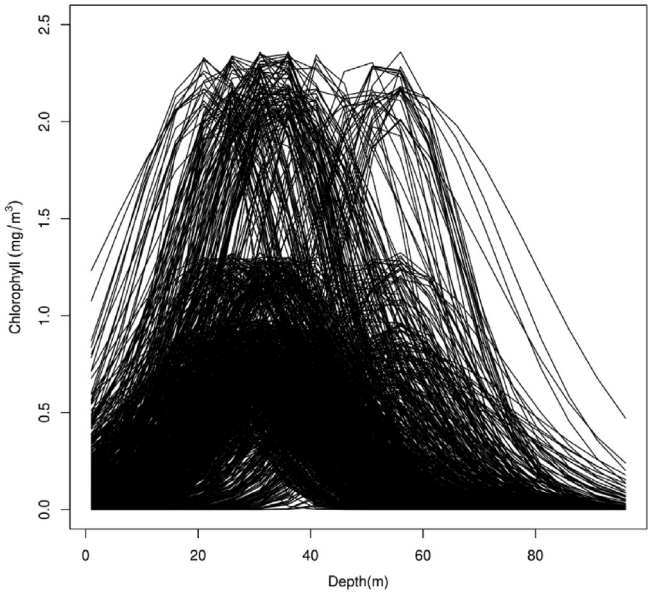

Fig. 13. Simulated chlorophyll profiles from Chloromax with random samples.

devised by combining the observed variability along with the multiple regression models. The model performs predictions on chlorophyll at each depth in the euphotic column, to predict the maxima of chlorophyll (Fig. 13).

$$\textit{Derived chlorophyll distribution over depth} = f(D) = \sigma t \times (-1.23) + par \times (-0.0044) + 30.41 \quad (6)$$

Where *sigma-t* (σt) is the density of seawater and can derive from relation with SST as described previously (32.74 + (−0.3277)× SST + RSE) and *par* is the photosynthetic Active Radiation (PAR), which can be derived using the exponential decay at $D_{\max}$, as done by (Fennel and Boss, 2003). The model was developed by equating Gaussian Eq. (1) with the derived chlorophyll distribution function Eq. (6).

That is equating (1) and (6)

$$Chl_{max}\, e^{\left[\frac{(-D-D_{max})}{Chl_{spd}}\right]^2} = \sigma t \times (-1.23) + par \times (-0.0044) + 30.41$$

$$Chl_{max} = \frac{30.41 + (-1.23) * \sigma_t + (-0.0044) * par}{e^{\left[\frac{(-D-D_{max})}{Chl_{spd}}\right]^2}} \quad (7)$$

where the chl_{max} is the chlorophyll maxima (value at SCM), D is the depth along the profile, D_{max} is the depth at which the maxima occur (which is a proxy to MLD for the NEAS spring) and Chl_{spd} is the spread of chlorophyll from maxima (chl_{max}), which is inconsistent parameter immensely controlled by biological factors like species compositions, or behaviors like photo/thermotaxis, etc. According to the observations in NEAS, Chl_{spd} is at around 22 m as estimated by the average of observations, and we have treated this as a constant in the model.

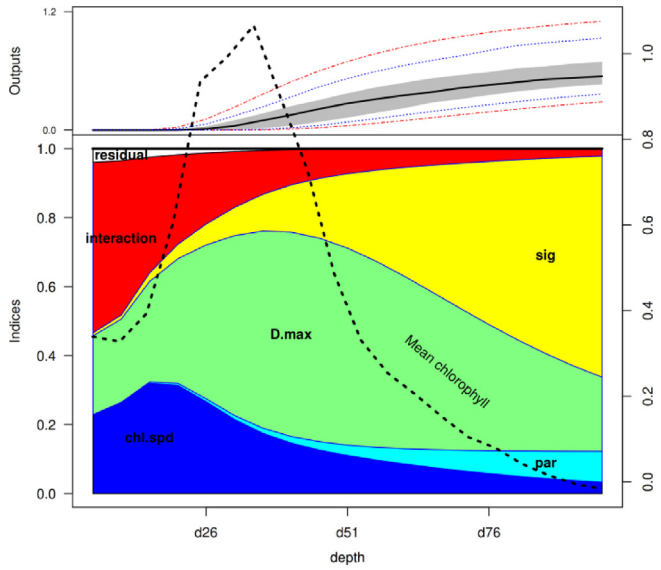

Fig. 14. Dynamics of the sensitivity indices of the *Chloromax* model from d = 5 to 100, with indices normalized to one. The upper subplot shows the extreme (tirets), inter-quartile (grey) and median (bold line) output values at all time steps. The lower subplot represents the sensitivity indices at all time steps for the main effects and first-order interactions. The overlay (- - -) shows mean chlorophyll from observation.

3.7. Model testing and Global Sensitivity Analysis (GSA)

The *Chloromax* is simulated with 1000 samples of random permutations of observed data, with bootstrap resampling methods. The output shows the model has only minor variations with the uncertainty of parameters. Sensitivity analysis (SA) is best appropriate to determine the contribution of each uncertain input factor to the uncertainty of a given output (Convertino et al., 2014). To quantify and compare the influence of uncertain parameters on the output of the model, Global Sensitivity Analysis (GSA is applied on the *Chloromax* as given in Eq. (8).

$$Chl_{max} = \frac{30.41 + (-1.23) * \sigma_t + (-0.0044) * par}{e^{\left[\frac{(-D-D_{peak})}{Chl_{spd}}\right]^2}} \quad (8)$$

The GSA was deployed using both univariate and multivariate approach for the current study. The analysis was conducted by putting a factorial design on the uncertain model parameters using the sequential univariate method, applied using R package "multisensi". Further, the sensitivity is more clarified by principal component analysis of model output (Fig. 14).

The upper subplot shows the extreme (dotted lines), inter-quartile (grey) and median (bold line) output values at all-time steps. The lower subplot represents the sensitivity indices at all-time steps for the main effects and the first-order interactions. The sensitivity indices at depth "d" are given by the lengths of the different colors along the y-axis of indices and dotted lines are chlorophyll profile derived from the Gaussian model (–) with the scale on right side of the plot. It is shown that the chlorophyll maxima at depths between 26 m and 46 m are getting more sensitive to the main effects of variables σt(sig), par(par), $D_{max\ (D.max)}$, and Chl_{spd} (chl.spd). It is observed that the chlorophyll maxima have occurred when the density parameter sigma (σt) is sensitive. The par is sensitive from the depth at which chlorophyll maxima occurs but comparatively lower than the sensitivity of σt. The parameters D_{max} and Chl_{spd} are derived components of the Gaussian model and are sensitive to the upper layers. The spreading factor Chl_{spd} is less sensitive and shallower than the depth of the maxima (D_{max}). The parameter D_{max} shows the highest sensitivity, which is found to be driven by σt than the par. At depths close to 100 m (−~76 m), the chlorophyll values are sensitive to σt as well as par, which is logical since the par is a very significant parameter for photosynthesis, and when it drops to the optimum levels in the deeper layers, becomes more sensitive to determine Chlorophyll Maxima (Fig. 15).

To obtain a more detailed view of the parameter's impact on the chlorophyll maxima multivariate sensitivity analysis is attempted, applying dimensional reduction and sensitivity analysis of each associated coefficients of decomposition. The best method identified to deploy this approach is Principle Component Analysis (PCA), and the analysis shows that the first principal component, which explains more than 95.9% of the inertia, captures essentially an average effect over depth. The lower subplots show the sensitivity indices, in which "σt" and

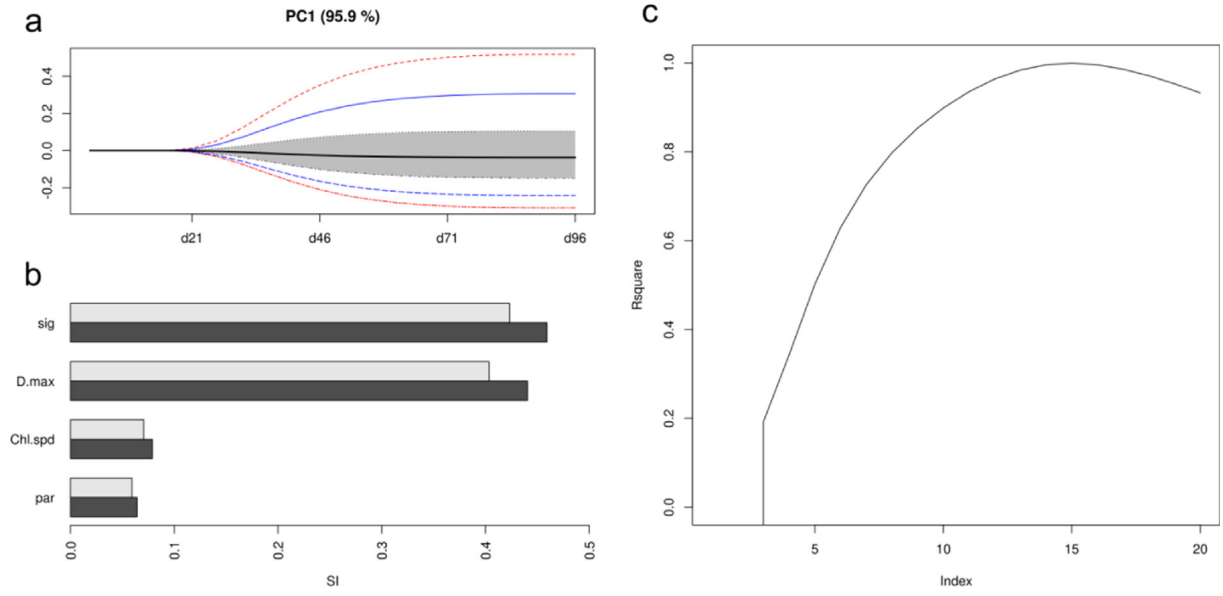

Fig. 15. a) Plot of PCA multivariate sensitivity analysis of the Chloromax model. Upper sub- plots: functional boxplots of the principal components, with depth on the x-axis and chlorophyll maxima contribution on the y-axis (red curves: extreme values, blue: 1/10 and 9/10 percentiles, grey area: inter-quartile, black: median). Lower subplots: sensitivity indices (light grey: first order indices, dark grey: total indices) b) Coefficients of determination of the output variables for the PCA multivariate sensitivity analysis of the Chloromax model on raw output data.

"D_{max}" are found to be the most prominent parameters and PAR is the least significant. The first principal component, which explains more than 90% of the inertia, captures essentially an average effect over depth. The proportions of variability accounted are quantified by R^2 coefficients of determination, provided the sensitivity analysis is based on ANOVA. It is significant that R^2 values are low for the upper depth variables due to low variance. The sensitivity analysis suggests that this model is effective on determining the effects of upper layer warming on column primary production and ecological interactions.

4. Conclusions

The present study attempts to infer the possible physical mechanisms contributing the SCM in the North Eastern Arabian Sea (NEAS) during initial Spring Inter-Monsoon (SIM) based on profiles from CTD and BioArgo, with the support of theoretical explanations. The region of study is the stereotype of a warm, stratified ocean, and the results from the present analysis gives an overview of the possible effects of fluid dynamic properties to regulate the settling of phytoplankton to form SCM of various species. Simulation experiments using Stokes equations bring out the fact that the fluid/seawater properties dominate over the shape or density of the organism in determining the settling depth in a light abundant system, resulting in contribution of non-motile phytoplankton cells (especially diatoms), to the SCM. A Numerical expression (named as *Chloromax*) is derived based on the analysis outputs and the sensitivity of the input parameters is validated based on Global Sensitivity Analysis (GSA). The results from the study would be a useful addition to address the possible changes in the production pattern of the tropical/subtropical ecosystems in the scenario of changing climate, which ultimately helps in efficient management of the resources.

Acknowledgment

The authors acknowledge Ministry of Earth Sciences, Govt. of India and Cochin University of Science and Technology (CUSAT), India for supporting the work and for providing facilities onboard FORV *Sagar Sampada* for in-situ measurements. Chlorophyll, SST and PAR data was retrieved from GSFC NASA. Shortwave radiation (swr, TropFlux net) and Eastward/Northward wind speed (ASCAT DATA) are taken from INCOIS-ESSO portal. Vertical Argo profiles of chlorophyll used for the study are received from INCOIS-ESSO Hyderabad, India. We thank Dr. Cara Wilson from NOAA, for a critical review and restructuring the paper. This is CMLRE contribution 107.

References

Bach, L.T., Riebesell, U., Sett, S., Febiri, S., Rzepka, P., Schulz, K.G., 2012. An approach for particle sinking velocity measurements in the 3–400 μm size range and considerations on the effect of temperature on sinking rates. Mar. Biol. 159 (8), 1853–1864.

Banerjee, P., Prasanna Kumar, S., 2014. Dust-induced episodic phytoplankton blooms in the Arabian Sea during winter monsoon. J. Geophys. Res. Oceans 119 (10), 7123–7138.

Behrenfeld, M.J., Boss, E.S., 2014. Resurrecting the ecological underpinnings of ocean plankton blooms. Annu. Rev. Mar. Sci. 6, 167–194.

Brock, J., Sathyendranath, S., Platt, T., 1993. Modelling the seasonality of subsurface light and primary production in the Arabian Sea. Mar. Ecol. Prog. Ser. 101 (3), 209–222.

Buitenhuis, E.T., Li, W.K.W., Vaulot, D., Lomas, M.W., Landry, M.R., Partensky, F., et al., 2012. Picophytoplankton biomass distribution in the global ocean. Earth Syst. Sci. Data 4 (1), 37–46.

Capotondi, A., Alexander, M.A., Bond, N.A., Curchitser, E.N., Scott, J.D., 2012. Enhanced upper ocean stratification with climate change in the CMIP3 models. J. Geophys. Res. Oceans 117 (C4).

Convertino, M., Muñoz-Carpena, R., Chu-Agor, M.L., Kiker, G.A., Linkov, I., 2014. Untangling drivers of species distributions: Global sensitivity and uncertainty analyses of MaxEnt. Environ. Model. Softw. 51, 296–309.

Cullen, J.J., 2015. Subsurface chlorophyll maximum layers: enduring enigma or mystery solved? Annu. Rev. Mar. Sci. 7 (1), 207–239.

De Boyer Montégut, C., Madec, G., Fischer, A.S., Lazar, A., Iudicone, D., 2004. Mixed layer depth over the global ocean: an examination of profile data and a profile based climatology. J. Geophys. Res. 109 (C12), C12003.

Dodge, J.D., Hart-Jones, B., 2009. The vertical and seasonal distribution of dinoflagellates in the North Sea. Bot. Mar. 17 (2), 113–117.

Dray, S., Dufour, A., 2007. The ade4 package: implementing the duality diagram for ecologists. J. Stat. Softw. 22, 1–20.

Falkowski, P.G., 1980. Light-Shade Adaptation in Marine Phytoplankton. In: Falkowski, P.G. (Ed.), Primary Productivity in the Sea. Springer, US, Boston, MA, pp. 99–119.

Fennel, K., Boss, E., 2003. Subsurface maxima of phytoplankton and chlorophyll: Steady-state solutions from a simple model. Limnol. Oceanogr. 48 (4), 1521–1534.

Gardner, W.D., Gundersen, J.S., Richardson, M.J., Walsh, I.D., 1999. The role of seasonal and diel changes in mixed-layer depth on carbon and chlorophyll distributions in the Arabian Sea. Deep Sea Res. Part II 46 (8–9), 1833–1858.

Goes, J.I., Thoppil, P.G., Gomes, H.D.R., Fasullo, J.T., 2005. Warming of the Eurasian landmass is making the Arabian sea more productive. Science (80-.) 308, 545–547.

Gomes, H.D.R., Goes, J.I., Matondkar, S.G.P., Parab, S.G., Al-Azri, A.R.N., Thoppil, P.G., 2008. Blooms of *Noctiluca miliaris* in the Arabian Sea—An in situ and satellite study. Deep Sea Res. Part I 55 (6), 751–765.

Gross, F., Zeuthen, E., 1948. The buoyancy of plankton diatoms: a problem of cell physiology. Proc. R. Soc. B: Biol. Sci. 135 (880), 382–389.

Harris, G.P., Heaney, S.I., Talling, J.F., 1979. Physiological and environmental constraints in the ecology of the planktonic dinoflagellate Ceratium hirundinella. Freshw. Biol. 9 (5), 413–428.

Harrison, P.J., Zingone, A., Mickelson, M.J., Lehtinen, S., Ramaiah, N., Kraberg, A.C., et al., 2015. Cell volumes of marine phytoplankton from globally distributed coastal data sets. Estuar. Coast. Shelf Sci. 162, 130–142.

Hasle, G.R., 1950. Phototactic vertical migration in marine dinoflagellates. Oikos 2 (2), 162–175.

Hay, B.J., McClain, C.R., Petzold, M., 1993. An assessment of the Nimbus-7/CZCS calibration for May 1986 using satellite and In situ data from the Arabian sea. Remote Sens. Environ. 43 (1), 35–46.

Huang, J., Xu, F., 2018. Observational evidence of subsurface chlorophyll response to mesoscale eddies in the north pacific. Geophys. Res. Lett. 45 (16), 8462–8470.

Huisman, J., Pham Thi, N.N., Karl, D.M., Sommeijer, B., 2006. Reduced mixing generates oscillations and chaos in the oceanic deep chlorophyll maximum. Nature 439 (7074), 322–325.

Jeffrey, S. W., Mantoura, R. F. C., Wright, S. W., International Council of Scientific Unions, & Unesco (Eds.). (1997). Phytoplankton pigments in oceanography: guidelines to modern methods. Paris: UNESCO Pub.

Jochem, F., 1995. Phototrophic picoplankton community structure in three different pelagic regimes in the Arabian Sea. Mar. Ecol. Prog. Ser. 117, 307–314.

Kassambara, A., Mundt, F. (2017). factoextra: Extract and Visualize the Results of Multivariate Data Analyses. Retrieved from https://CRAN.R-project.org/package=factoextra.

Kelley, D., Richards, C., & SCOR/IAPSO, W. (2017). gsw: Gibbs Sea Water Functions. Retrieved from https://CRAN.R-project.org/package=gsw.

Kim, W., Yeh, S.-W., Kim, J.-H., Kug, J.-S., Kwon, M., 2011. The unique 2009–2010 El Niño event: A fast phase transition of warm pool El Niño to La Niña. Geophys. Res. Lett. 38 (15).

Krey, J., 1976. Phytoplankton production: atlas of the International Indian Ocean Expedition. Kiel:; Paris: Institut für Meereskunde an der Universität Kiel;;Available from. Intergovernmental Oceanographic Commission.

Kumar, S.P., Ramaiah, N., Gauns, M., Sarma, V.V.S.S., Muraleedharan, P.M., Raghukumar, S., et al., 2001. Physical forcing of biological productivity in the Northern Arabian Sea during the Northeast Monsoon. Deep Sea Res. Part II 48 (6), 1115–1126.

Lotliker, A.A., Baliarsingh, S.K., Trainer, V.L., Wells, M.L., Wilson, C., Udaya Bhaskar, T.V.S., et al., 2018. Characterization of oceanic *Noctiluca* blooms not associated with hypoxia in the Northeastern Arabian Sea. Harmful Algae 74, 46–57.

Macías, D., Rodríguez-Santana, Á., Ramírez-Romero, E., Bruno, M., Pelegrí, J.L., Sangrà, P., et al., 2013. Turbulence as a driver for vertical plankton distribution in the subsurface upper ocean. Scientia Marina 77 (4), 541–549.

Matondkar, S. G. P., Parab, S., & Dwivedi, R. M. (2006). Seasonality in subsurface chlorophyll maxima in the Arabian Sea: detection by IRS-P4/OCM and implication of it to primary productivity (Vol. 6406, p. 64060X). Presented at the Society of Photo-Optical Instrumentation Engineers (SPIE) Conference Series.

Moore, J.K., Villareal, T.A., 1996. Size-ascent rate relationships in positively buoyant marine diatoms. Limnol. Oceanogr. 41 (7), 1514–1520.

Kumar, S.P., Prasad, T.G., 1996. Winter cooling in the northern Arabian Sea. JGOFS (INDIA) 71 (11), 834–841.

Ravichandran, M., Girishkumar, M.S., Riser, S., 2012. Observed variability of chlorophyll-a using Argo profiling floats in the southeastern Arabian Sea. Deep Sea Res. Part I: Oceanogr. Res. Pap. 65, 15–25.

Richardson, K., Beardall, J., Raven, J.A., 1983. Adaptation of unicellular algae to irradiance: an analysis of strategies. New Phytol. 93 (2), 157–191.

Rosario Gomes, H., Matondkar, S.G.P., Parab, S.G., Goes, J.I., Pednekar, S., Al-Azri, A.R.N., Thoppil, P.G., 2009. Unusual blooms of green *Noctiluca miliaris* (Dinophyceae) in the Arabian Sea during the winter monsoon. Washington DC American Geophysical Union Geophysical Monograph Series 185, 347–363.

Valiela, I., 1995. Factors Affecting Primary Production. In: Marine Ecological Processes. New York, NY, Springer, New York, pp. 36–79.

Wang, S., Li, S., Hu, J., Geng, B., 2016. Experiments in optimizing simulations of the subsurface chlorophyll maximum in the South China Sea. J. Mar. Syst. 156, 1–15.